Journal of Applied Polymer Science

Improvement of the thermal transport performance of a poly(vinylidene fluoride) composite film including silver nanowire

Zhao Li, Li Zhang, Rong Qi, Fan Xie, Shuhua Qi
Department of Applied Chemistry, School of Science, Northwestern Polytechnical University, Xi'an 710072, People's Republic of China
Correspondence to: S. Qi (E-mail: qishuhuanwpu@163.com)

ABSTRACT: The miniaturization trend of electronic devices requires that components have a high heat dissipation in industrial applications and in daily life. In this context, a highly thermally conductive film was fabricated with silver nanowire (AgNW) and poly(vinylidene fluoride) (PVDF) with a bar-coating method. The thermal transport performance and mechanism of the AgNW/PVDF composite film were investigated. The through-plane and in-plane thermal conductivity of the AgNW/PVDF composite film reached 0.31 and 1.61 W m^{-1} K^{-1}, respectively; these values far exceeded those of the pristine PVDF film. The experiment illustrated that the thermally conductive pathways formed successfully in the PVDF substrate with the addition of AgNW, and the heat tended to transfer along the thermally conductive pathway rather than along the PVDF substrate. © 2016 Wiley Periodicals, Inc. J. Appl. Polym. Sci. **2016**, *133*, 43554.

KEYWORDS: composites; films; nanoparticles; nanowires and nanocrystals; thermal properties

Received 16 December 2015; accepted 18 February 2016
DOI: 10.1002/app.43554

INTRODUCTION

Electronic devices, such as mobile phones, tablets, and laptop computers, have become more and more familiar in our day-to-day lives.[1] The miniaturization trend of electronic devices requires that components have a high heat dissipation.[2] There is no doubt that the operating temperature affects the reliability of electronic devices.[3] It is urgent to improve this property of electronic devices because of the demand for a high thermal conductivity in traditional materials. The thermal conductivity of polymers is usually approximately 0.1 W m^{-1} k^{-1}; this greatly restricts their use as traditional thermally conductive materials. To overcome these drawbacks, various novel materials of high thermal conductivity, such as silver nanowire (AgNW), silver, carbon nanotubes,[4] graphene,[5,6] and metal nanostructures,[7] are used as thermal transfer media to fill the polymer matrix. These fillers can significantly increase the thermal conductivity of polymers and can simultaneously enhance the electrical conductivity of the polymer.[8] In addition to the high thermal conductivity, there are other advantageous properties in these new types of fillers, including excellent mechanical properties, light weight, and excellent chemical properties. These good performances can cater to the special demand for lightweight and miniaturized electronic materials.

As we know, highly thermally conductive materials can meet the heat-transfer demand of the majority of electronic devices. Thus, some ceramic fillers are blended with the polymer substrate as thermally conductive fillers; these fillers include boron nitride,[9,10] aluminum nitride,[11] silicon carbide,[12] and alumina. However, a high volume fraction of ceramic fillers, generally exceeding 60%, is necessary to obtain a high thermal conductivity in the composite. Also, these fillers seriously affect the mechanical properties and flexibility of the polymer composite for practical applications. The thermal conductivity of polymers filled with ceramic fillers is lower because of the thermal resistance at the interface between the fillers and the polymer.[13] Metallic nanowires, such as AgNW, are very promising candidates for the fabrication of transparent and flexible films[14] to replace traditional materials. AgNW is an excellent candidate for films that are transparent and flexible and have a high electrical and thermal conductivity because of their high aspect ratio and excellent electrical, optical, magnetic, and thermal properties. More and more researchers have revealed various applications based on AgNW; these applications include transparent electrodes in thin-film solar cells,[15,16] organic light-emitting diodes,[17] touch panels,[18] fuel cells,[19] and stretchable electronic devices.[20,21]

Additional Supporting Information may be found in the online version of this article

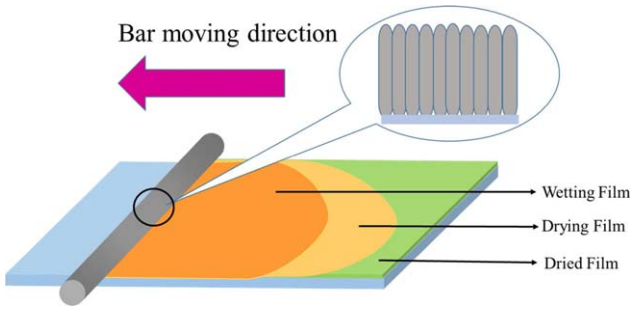

Figure 1. Schematic description of the wire bar-coating process. [Color figure can be viewed in the online issue, which is available at wileyonlinelibrary.com.]

Because poly(vinylidene fluoride) (PVDF) is a partially fluorinated polymer, it exhibits superior electrochemical and thermal stability and a great potential for application in sensors, piezoelectric materials,[22] and biomedical fields.[23] AgNW, as a novel type of filler, has been added to PVDF. The AgNW tend to aggregate without other additives to prevent their aggregation because of their nanometer properties.[24] Previous research has shown that silica nanoparticles can improve the thermomechanical properties and other properties. In this study, a flexible and highly thermally conductive film was fabricated via a thermally assisted evaporation phase separation. The PVDF particles dissolved in *N,N*-dimethylformamide (DMF) and formed a PVDF/DMF homogeneous phase solution. The AgNW/PVDF composite film was fabricated via a mixture solution, which was composed of self-made AgNW, a PVDF/DMF homogeneous phase solution, and silica nanoparticles.

In this article, we report on a simple wire-bar-coating process as a suitable method for the deposition of a homogeneous solution[25] composed of AgNW and a PVDF/DMF precursor solution. The AgNW/PVDF film was obtained from a semitransparent polymer homogeneous solution by intermittent and multiple wire-bar-coating processes on a 6-cm glass or plastic substrate. The film thickness was mainly affected by the solution of the polymer, the quality of bar, the diameter of the wound metal wires on the bar, and the coating speed. In this study, the glass was coated on the solution, which was precisely controlled at 50 μL by pipette each time; we repeated the previous operation every 60 s, and each operation was repeated for a total of 10 times.[26] Interestingly, the polymer solution and slide cleaned with deionized water and ethyl alcohol sequentially had a perfect spreadability. The film represented three forms: the dried film, drying film, and wetting film in the back of the bar movement; this was attributed to the style of intermittent and multiple coatings (Figure 1).

EXPERIMENTAL

Fabrication of AgNW

AgNW was synthesized with a hydrothermal process, which set glycerol as the reductant and solvent, PVP as the surfactant and structure-directing agent, and silver nitrate as the precursor, respectively. Amounts of 5.86 g of PVP and 90 mL of glycerol were dissolved absolutely in a beaker at 50 °C, and then, the temperature of the solution was reduced to 20 °C. At approximately 1 h, when the temperature was stable, 10 mL of a 59 g/L sodium chloride solution was added to the preceding solution, and it was reacted for 15 min under mechanical agitation. Subsequently, 90 mL of a 17.5 g/L silver nitrate solution was added to the beaker at a rate of 10 mL/min. The solution was heated to 210 °C rapidly, and about 30 min later, the solution became dark gray. Later, it became bright gray. These phenomena indicted that the AgNW was fabricated successfully. The solution was cooled down to 20 °C and centrifuged at 8000 rpm to remove glycerol, PVP, and other impurities. Finally, the AgNW was dispersed into absolute ethyl alcohol. The process of fabrication of AgNW is detailed in the Supporting Information (Figure S1, Supporting Information).

Bar Coating of the AgNW/PVDF Composite Film

As illustrated in Figure 2, the amounts of AgNW/PVDF precursor solution (the processes of fabrication are shown in Figure S2, Supporting Information) were controlled precisely via pipette and transferred onto the precleaned glass substrate.[27] The AgNW/PVDF prefabricated film was fabricated successfully via the wire-bar-coating method with the wire-wound bar (diameter = 12 mm) and the wire coil (diameter = 100 μm) at a bar speed of 40 mm/s. The glass slide attached to the prefabricated film was dried in a vacuum-drying oven at 60 °C for 4 h. When the DMF was entirely volatilized, the AgNW/PVDF composite film was obtained and was then peeled off of the glass substrate.

Characterization

The surface morphologies of the AgNW and AgNW/PVDF film were characterized with scanning electron microscopy (SEM; JSM-6360LV). The structural characterization of the film was obtained with X-ray diffraction on an X'Pert MPD Pro Advanced diffractometer with Cu Kα radiation ($\lambda = 1.54056$). The thermal diffusion coefficient of the AgNW/PVDF film was measured with the laser flash method (LFA447, Netzsch, Germany) at room temperature, and the heat-conduction effect of the AgNW/PVDF film was characterized with an IR system (Thermal Imaging Electrical Technology Co., Ltd., Shanghai, China).

RESULTS AND DISCUSSION

Microstructure of AgNW

Figure 3(a,b) shows SEM images of the AgNW film and AgNW/PVDF composite film. SEM images indicated that AgNW was successfully prepared. The photograph of the AgNWs revealed

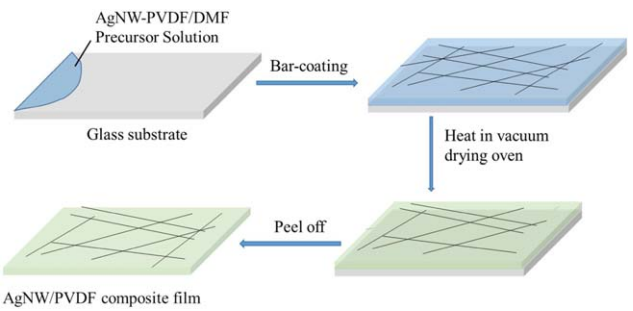

Figure 2. Schematic illustration of the fabrication procedure of the AgNW/PVDF composite film. [Color figure can be viewed in the online issue, which is available at wileyonlinelibrary.com.]

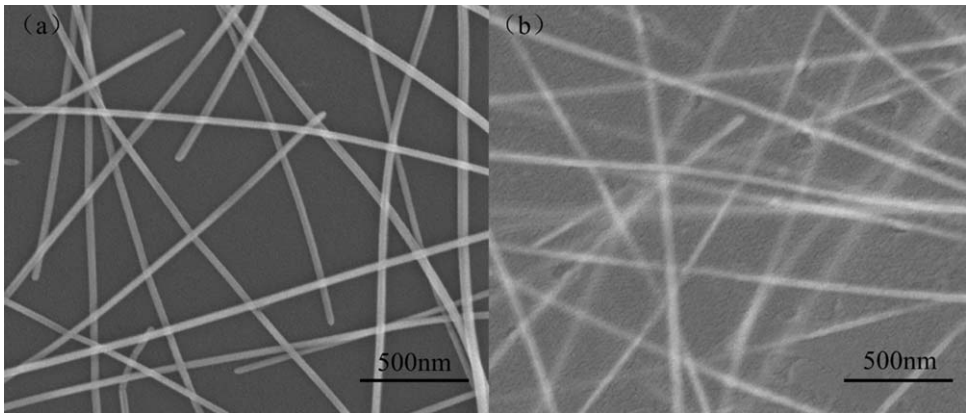

Figure 3. SEM images of the synthesized AgNW (a) on a glass substrate and (b) embedded in a PVDF matrix.

that the average length of AgNW approximately reached 15 μm, and the average diameter of AgNW reached 70 nm; this was characterized by SEM. The AgNW was dispersed uniformly in the PVDF/DMF precursor solution with the help of silica nanoparticles, as previous research reported that AgNW tended to aggregate without silica nanoparticles and dispersed well when the solution contained silica nanoparticles.[28]

Crystal Structure

AgNW was expected to be an ideal filling material for the thermally conductive film because of its intrinsic thermal conductivity and large ratio.[29] AgNW/PVDF composite films at different volume fractions were prepared, and their thermal performances were measured systematically. PVDF, as a kind of partially fluorinated polymer, was chosen as the matrix because of its good crystallization and good film-forming properties.

Figure 4 illustrates the X-ray diffraction spectra of the pristine PVDF film and 5, 10, 15, 20, and 25 vol % AgNW/PVDF films, respectively. Four diffraction peaks, labeled by red rectangles, were observed at 38.5, 44.5, 65.0, and 78.1°; these were assigned to the (111), (200), (220), and (311) reflections, respectively, of the surface-centered cubic structure of metallic silver according to the Silver Joint Committee on Powder Diffraction Standards Database. The additional peak, labeled by a black rectangle, was observed at 20.8°, and it was attributed to the β phase of PVDF. No other peaks were observed; this indicated the absence of other impurities in the AgNW/PVDF composite film. The plot revealed that AgNW had no effect on the crystallization of the AgNW/PVDF composite film.

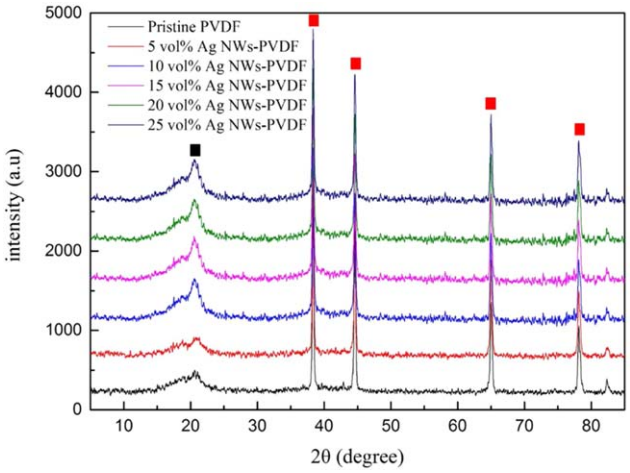

Figure 4. X-ray diffraction of the pristine PVDF film and AgNW/PVDF films with different volume fractions. [Color figure can be viewed in the online issue, which is available at wileyonlinelibrary.com.]

Thermal Properties

To illustrate the thermally conductive properties of the AgNW/PVDF film, the thermal diffusion coefficient was measured via the laser flash method, and the heat leakage correction was amended by the Cowan model. The experiment indicated that the thermal diffusion coefficient increased with increasing quality percentage of AgNW. The thermal conductivity was acquired according to the following equation[30]:

$$\alpha = \frac{k}{\rho c}$$

where k is the thermal conductivity, α is the thermal diffusivity, c is the specific heat capacity, and ρ is the density. The thermal conductivity and thermal diffusion coefficient did not present a linear relationship as the slightly changing density of the AgNW/PVDF film. The reason behind this phenomenon was that the specific heat and density of the AgNW/PVDF film showed slight changes with the fraction increase in AgNW.

As shown in Figure 5(a,b), the in-plane thermal conductivity and through-plane thermal conductivity were calculated on the basis of the thermal diffusivity, specific heat capacity, and density. For the AgNW/PVDF composite film, the data indicated that both the in-plane thermal conductivity and the through-plane thermal conductivity exceeded those of the pristine PVDF film. The IR image was captured by an IR camera [Figure 5(c)] on the basis of the IR image monitoring system, which is shown in Figure 5(d). For the IR camera, a similar or identical color represented similar or identical temperatures. Compared Figure 5(e,f), the IR image indicated that the heat-transfer speed of the AgNW/PVDF composite film was faster than that of the pristine PVDF film.

Thermal Conduction Mechanism

As we know, the free-electron theory of electron conduction is a main heat-transfer mechanism in metal solids. Lots of energy is

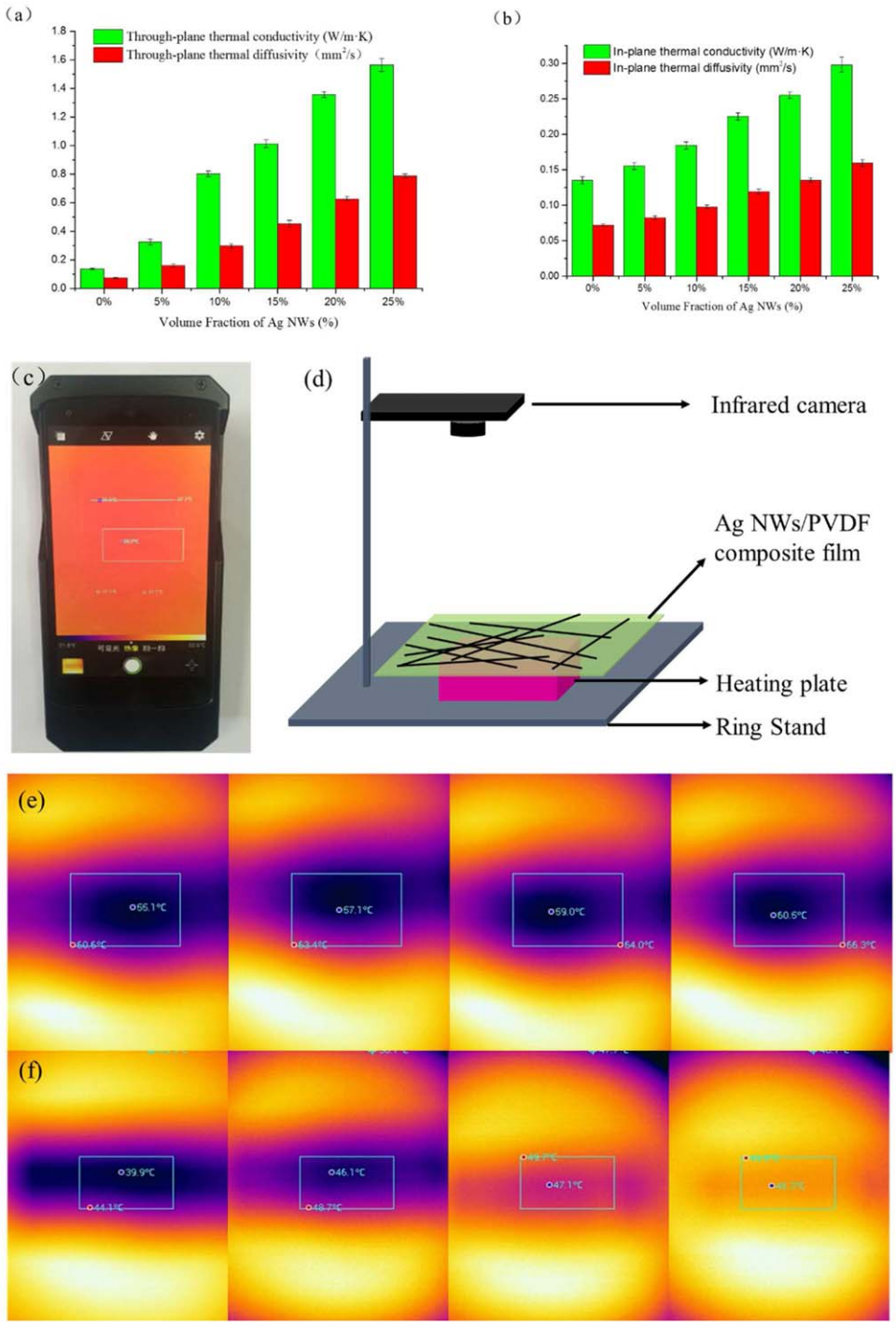

Figure 5. (a) Through-plane thermal conductivity and through-plane thermal diffusivity at different volume fractions. (b) In-plane thermal conductivity and in-plane thermal diffusivity at different volume fractions. (c) IR camera. (d) Schematic diagram of monitoring via the IR camera. (e) Thermal images captured from the pristine PVDF film with the IR camera. (f) Thermal images captured from the AgNW/PVDF composite film with the IR camera. [Color figure can be viewed in the online issue, which is available at wileyonlinelibrary.com.]

used in the process of migration of free electrons with abundant charge, so the heat conductivity of metals is very high. However, for nonmetals and polymers, lattice thermal conduction is the dominant thermal conduction mechanism. The vibrations of atoms are not independent of each other but are rather strongly coupled with neighboring atoms. In this context, AgNW, as a novel filler, disperses in the polymer precursor solution and prepares the AgNW/PVDF composite film. As illustrated in Figure 5(a,b), the thermal conductivity increased with the volume fractions of AgNW in the precursor solution. When a small amount of AgNW was added to the precursor solution, the AgNW was almost covered by the polymer. This was similar to the

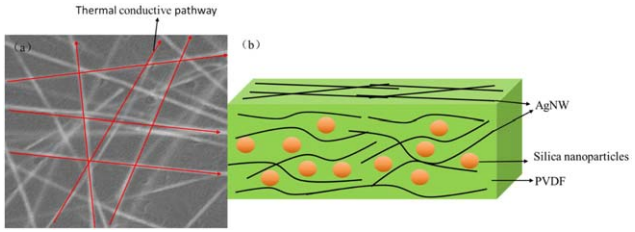

Figure 6. (a) SEM image of the AgNW/PVDF composite film forming a thermally conductive pathway. (b) Dispersion principle diagram of AgNW in the AgNW/PVDF composite film. [Color figure can be viewed in the online issue, which is available at wileyonlinelibrary.com.]

sea-island system in a polymer blending system. When the volume fraction of AgNW reached 15%, the through-plane thermal conductivity of the AgNW/PVDF composite film increased rapidly to 1.04 W m^{-1} K^{-1}. It was apparent from the SEM image [Figure 6(a)] that the thermally conductive pathways formed successfully because of addition of vast AgNW, which was labeled with the red line with the arrow. The experiment showed that the heat was transferred along the thermally conductive pathways (AgNW) rather than along the polymer substrate. For the AgNW/PVDF composite film, because the high length–diameter ratio of the AgNW, the through-plane thermal conductivity far exceeded the in-plane thermal conductivity; the thermal diffusion coefficient of the AgNW/PVDF composite film also showed the same trend. Figure 6(b) shows the dispersion mechanism of AgNW in the polymer matrix. The AgNW was dispersed uniformly in the PVDF precursor solution with the help of silica nanoparticles.

CONCLUSIONS

In conclusion, a highly thermally conductive film was fabricated successfully, and its thermal performance was researched. Compared with the pristine PVDF film, the AgNW/PVDF composite film exhibited an excellent thermal conductivity. The through-plane and in-plane thermal conductivities of the AgNW/PVDF composite film reached 0.31 and 1.61 W m^{-1} K^{-1}, respectively; these values far exceeded those of the pristine PVDF film. The surface temperature indicated that the heat-transfer speed of the AgNW/PVDF composite film was obviously faster than that of the pristine PVDF film; this was attributed to the thermally conductive pathways in the AgNW/PVDF composite film.

REFERENCES

1. Li, J.; Liang, J.; Li, L.; Ren, F.; Hu, W.; Li, J.; Qi, S.; Pei, Q. *ACS Nano* **2014**, *128*, 74.
2. Xia, J.; Zhang, G.; Deng, L.; Yang, H.; Sun, R.; Wong, C.-P. *RSC Adv.* **2015**, *193*, 15.
3. Hwang, Y.; Kim, M.; Kim, J. *RSC Adv.* **2014**, *170*, 15.
4. Tenent, R. C.; Barnes, T. M.; Bergeson, J. D.; Ferguson, A. J.; To, B.; Gedvilas, L. M.; Heben, M. J.; Blackburn *J. L. Adv. Mater.* **2009**, *32*, 10.
5. Rana, K.; Singh, J.; Ahn, J.-H. *J. Mater. Chem. C* **2014**, *26*, 46.
6. Hwang, J. O.; Park, J. S.; Choi, D. S.; Kim, J. Y.; Lee, S. H.; Lee, K. E.; Kim, Y.-H.; Song, M. H.; Yoo, S.; Kim, S. O. *ACS Nano* **2011**, *6*, 159.
7. Rathmell, A. R.; Bergin, S. M.; Hua, Y. L.; Li, Z. Y.; Wiley, B. *J. Adv. Mater.* **2010**, *22*, 3558.
8. Qian, R.; Yu, J.; Wu, C.; Zhai, X.; Jiang, P. *RSC Adv.* **2013**, *173*, 73.
9. Li, T.-L.; Hsu, S. L.-C. *J. Phys. Chem. B* **2010**, *68*, 25.
10. Yan, W.; Zhang, Y.; Sun, H.; Liu, S.; Chi, Z.; Chen, X.; Xu, J. *J. Mater. Chem. A* **2014**, *209*, 58.
11. Agrawal, A.; Satapathy, A. *Compos. A* **2014**, *63*, 51.
12. Cao, J.-P.; Zhao, X.; Zhao, J.; Zha, J.-W.; Hu, G.-H.; Dang, Z.-M. *ACS Appl. Mater. Interfaces* **2013**, *69*, 15.
13. Shimazaki, Y.; Hojo, F.; Takezawa, Y. *Appl. Phys. Lett.* **2008**, *133*, 309.
14. Hu, L.; Kim, H. S.; Lee, J.-Y.; Peumans, P.; Cui, Y. *ACS Nano* **2010**, *29*, 55.
15. Kang, M.-G.; Park, H. J.; Ahn, S. H.; Xu, T.; Guo, L. J. *IEEE Sel. Top. Quantum Electron.* **2010**, *180*, 7.
16. Gaynor, W.; Lee, J.-Y.; Peumans, P. *ACS Nano* **2009**, *4*, 30.
17. Zeng, X. Y.; Zhang, Q. K.; Yu, R. M.; Lu, C. Z. *Adv. Mater.* **2010**, *22*, 4484.
18. Lee, J.; Lee, P.; Lee, H.; Lee, D.; Lee, S. S.; Ko, S. H. *Nanoscale* **2012**, *4*, 6408.
19. Chang, I.; Park, T.; Lee, J.; Lee, H. B.; Ji, S.; Lee, M. H.; Ko, S. H.; Cha, S. W. *Int. J. Hydrogen Energy* **2014**, *39*, 7422.
20. Lee, P.; Ham, J.; Lee, J.; Hong, S.; Han, S.; Suh, Y. D.; Lee, S. E.; Yeo, J.; Lee, S. S.; Lee, D. *Adv. Funct. Mater.* **2014**, *24*, 5671.
21. Lee, P.; Lee, J.; Lee, H.; Yeo, J.; Hong, S.; Nam, K. H.; Lee, D.; Lee, S. S.; Ko, S. H. *Adv. Mater.* **2012**, *24*, 3326.
22. Kang, G.-D.; Cao, Y.-M. *J. Membr. Sci.* **2014**, *463*, 145.
23. Chu, B.; Zhou, X.; Ren, K.; Neese, B.; Lin, M.; Wang, Q.; Bauer, F.; Zhang, Q. *Science* **2006**, *313*, 334.
24. Nam, S.; Cho, H. W.; Lim, S.; Kim, D.; Kim, H.; Sung, B. J. *ACS Nano* **2013**, *7*, 851.
25. Khim, D.; Han, H.; Baeg, K. J.; Kim, J.; Kwak, S. W.; Kim, D. Y.; Noh, Y. Y. *Adv. Mater.* **2013**, *25*, 4302.
26. Lee, W.; Hong, C. T.; Kwon, O. H.; Yoo, Y.; Kang, Y. H.; Lee, J. Y.; Cho, S. Y.; Jang, K. S. *ACS Appl. Mater. Interfaces* **2015**, *7*, 6550.
27. Lee, W. J.; Park, W. T.; Park, S.; Sung, S.; Noh, Y. Y.; Yoon, M. H. *Adv. Mater.* **2015**, *27*, 5043.
28. Nam, S.; Cho, H. W.; Lim, S.; Kim, D.; Kim, H.; Sung, B. J. *ACS Nano* **2012**, *7*, 851.
29. Wang, S.; Cheng, Y.; Wang, R.; Sun, J.; Gao, L. *ACS Appl. Mater. Interfaces* **2014**, *6*, 6481.
30. Wang, Z.; Kriegs, H.; Wiegand, S. *J. Phys. Chem. B* **2012**, *116*, 7463.